Finite-range effects in the πNN,πNΔ and π ΔΔ vertices

1979 J. Phys. G: Nucl. Phys. 5 223

(http://iopscience.iop.org/0305-4616/5/2/010)

J. Phys. G: Nucl. Phys., Vol.5, No.2, 1979. Printed in Great Britain

Finite-range effects in the πNN, πNΔ and πΔΔ vertices†

M Dillig‡ and M Brack§
Department of Physics, SUNY, Stony Brook, NY 11794, USA

Received 2 February 1978, in final form 11 August 1978

Abstract. The structure of the πNN, πNΔ and $\pi\Delta\Delta$ vertices is investigated in a microscopic model. Besides the inclusion of a consistent set of diagrams in lowest order, higher-order corrections from the strongly dominating $\pi\rho$ triangle diagram are included by solving a set of coupled integral equations, thereby allowing for the excitation of nucleonic and isobaric intermediate states. The resulting cut-off masses in a monopole parametrisation are $\gtrsim 8m_\pi$ for the πNN and $\gtrsim 6m_\pi$ for the πNΔ vertex.

The structure of the πNN vertex and its continuation off the energy shell—which is of considerable influence on processes involving high momentum transfers—is presently not very well understood. Most frequently, this structure is exploited by comparing experimental information from peripheral processes with predictions of simple one-pion-exchange models; the discrepancies between theory and expèriment are then understood as the effect of the finite range of the πNN vertex. As a result of such investigations a very small cut-off mass for a monopole parametrisation of the πNN form factor

$$F_\pi(q^2) = (\Lambda^2 - m_\pi^2)/(\Lambda^2 - q^2) \tag{1}$$

with $\Lambda \lesssim 5m_\pi$ is found (Ferrari and Selleri 1962, Mann *et al* 1973, Bongardt *et al* 1974). Such a result differs drastically from information about $F_\pi(q^2)$ as extracted from fits of NN phase-shifts, which favour a cut-off mass $\Lambda \gtrsim 10m_\pi$ (Bryan and Scott 1969, Erkelenz 1974, Holinde and Machleidt 1976). This striking discrepancy, combined with the fact that the determination of the πNN vertex structure directly from experimental data always involves the problem of how to subtract competing background processes, makes a microscopic investigation of the πNN vertex both worthwhile and promising.

In the language of perturbation theory, the off-shell behaviour of the πNN vertex is determined by the sum of vertex and self-energy corrections, which carry the correct quantum numbers and which, on the energy shell, reduce to the experimental pion mass and coupling constant. Typical contributions to this infinite series are listed schematically in figure 1: the 'dressed' πNN vertex is built up by the bare vertex (a) (which has, by definition, zero range) plus contributions from triangle diagrams (b, c) and self-energy corrections to the nucleon (d) and the pion propagator (e, f). In our calculation we consider in a first step only these diagrams; higher-order corrections, such as the diagrams (g, h), are neglected: for pion momenta q near the energy shell, i.e. $q^2 < m_\rho^2$, they should be

† Work supported in part by USERDA contract E(11-1)-3001.
‡ Present address: Institute for Theoretical Physics, University Erlangen–Nürnberg, Erlangen, Germany.
§ Permanent address: Institute for Theoretical Physics, University of Regensburg, Regensburg, Germany.

0305-4616/79/020223+06\$01.00

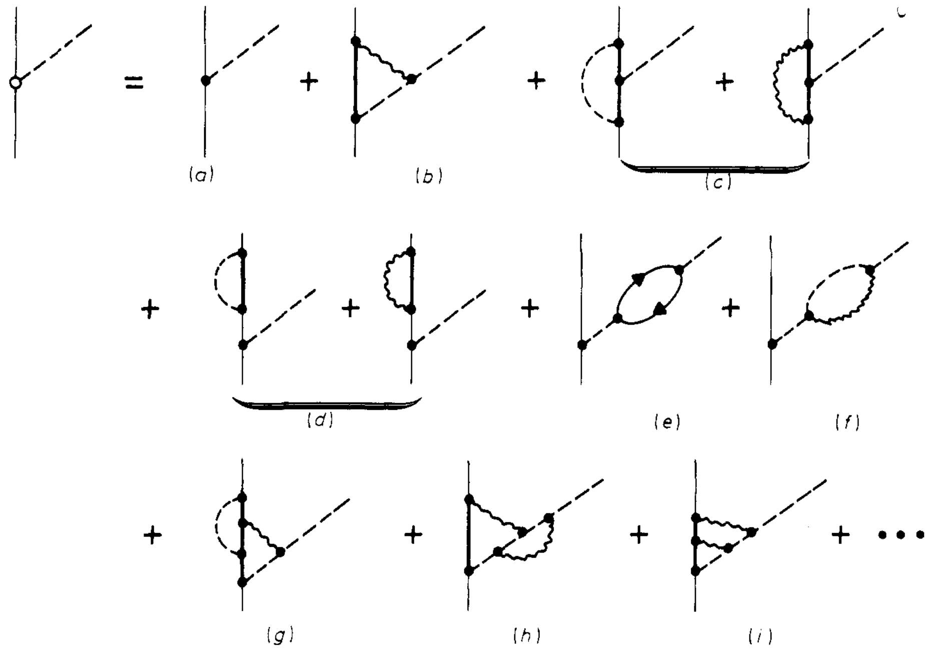

Figure 1. Schematical decomposition of the πNN vertex into the bare vertex (a), triangle diagrams (b, c) and propagator corrections (d–f). Some higher-order contributions are indicated in diagrams (g–i). In the figure full lines denote nucleons, broken lines pions and wavy lines σ or ρ mesons. The heavy intermediate baryon lines represent either nucleons or, when allowed by the selection rules, Δ isobars.

suppressed either by the large mass of the exchanged mesons (which corresponds in the framework of dispersion theory to the conventional assumption that contributions from distant cuts are small) or by the small coupling constants involved (for example, estimations indicate that the—low-mass—contributions from the 3π and 5π continuum are small (Pagels 1969, 1975)). Consequently, only contributions from mesonic $\pi\sigma$ and $\pi\rho$ intermediate states are considered in our model.

The restriction to pion momenta near the energy shell to some extent also justifies selecting from different Lagrangians, which are equivalent for on-shell pions, of the most simple ansatz: in combination with the self-consistent evaluation of the finite-range corrections (as formulated below), we then expect a very moderate dependence of the results on the particular structure of the effective Lagrangians which enter into the calculation.

The inclusion of diagrams (a)–(f) in figure 1 allows the formulation of a gauge-invariant description for the ρ, π, N system. It is easily verified that for an interaction Lagrangian (Yang and Mills 1954)

$$L_{\rho\pi N} = \mathrm{i}g_\rho \bar{\psi}_N \left\{ j_\mu + \frac{\kappa}{2M}\phi_{\mu\nu}q_\nu \right\} \psi_N(\tau \cdot \phi^\rho_\mu) + 2g_\rho(\partial_\mu \phi^\pi \times \phi^\pi) \cdot \phi^\rho_\mu - g^2_\rho(\phi^\pi \times \phi^\rho_\mu) \times \phi^\pi \cdot \phi^\rho_\mu \tag{2}$$

the resulting current is conserved; this allows us to eliminate the troublesome, highly divergent gauge term in the ρ propagator, which is then reduced to

$$D^\rho_{\mu\nu}(q^2) = g_{\mu\nu}/(q^2 - m^2_\rho). \tag{3}$$

In actual calculations the last term in equation (2) was dropped since its contribution is suppressed both by the coupling and the mass structure of the resulting intermediate state.

The evaluation of the diagrams (*a*)–(*f*) in figure 1 was performed in the framework of conventional (Feynman) perturbation theory. Compared with a dispersion theoretical approach which—assuming a well behaved analytical structure for the vertex function in the q^2 plane—starts from the relation (Pagels 1969, Braathen 1972, Durso *et al* 1977)

$$F_\pi(q^2) = 1 + \frac{1}{\pi}\int_{(m_1+m_2)^2}^{\infty} \mathrm{Im}\, F_\pi(q'^2)/(q'^2 - q^2)\,\mathrm{d}q'^2, \tag{4}$$

where m_1, m_2 refer to the exchanged particles (subtractions are included easily), the explicit evaluation of Feynman diagrams has the basic advantage that the resulting integrals over the intermediate momenta of the exchanged particles are dominated by much smaller momenta than the corresponding dispersion integrals and are therefore much less dependent on the cut-off (Durso *et al* 1977). Therefore it is also a good approximation to use the nonrelativistic forms of the various coupling Lagrangians and the intermediate baryon propagators, provided that the fully relativistic meson propagators are included. We therefore use the Lagrangians

$$L_{\pi \mathrm{BB}} = \frac{f_{\pi \mathrm{BB}}}{m_\pi}(\boldsymbol{\Sigma}_S \boldsymbol{q})(\boldsymbol{\Sigma}_T \boldsymbol{\phi}_\pi) \tag{5a}$$

and

$$L_{\rho BB} = \frac{f_{\rho BB}}{m_\rho}\varepsilon(\boldsymbol{\Sigma}_S \times \boldsymbol{q})(\boldsymbol{\Sigma}_T \boldsymbol{\phi}_\rho) \tag{5b}$$

with $\boldsymbol{\Sigma}_{S,T}$ defined by $\langle \frac{1}{2}\|\Sigma_0\|\frac{1}{2}\rangle = \sqrt{6}$, $\langle \frac{3}{2}\|\Sigma_1^\dagger\|\frac{1}{2}\rangle = 2$ and $\langle \frac{3}{2}\|\Sigma_2\|\frac{3}{2}\rangle = 2\sqrt{15}$ (Brown and Weise 1975). The coupling constants are $f_\pi^2/4\pi = 0{\cdot}08$ and $f_\rho^2/4\pi = g_\rho^2/4\pi(1+\kappa)^2(m_\rho/2m_\mathrm{N})^2$ with $m_\rho = 765$ MeV, $g_\rho^2/4\pi = 0{\cdot}52$ and $\kappa \simeq 6$ (Iachello *et al* 1973); the σ parameters are specified as $f_{\sigma\pi\pi}^2/4\pi = 0{\cdot}33 m_\mathrm{N}^2$ and $g_{\sigma\mathrm{NN}}^2/4\pi = 2{\cdot}06$ with $m_\sigma = 750$ MeV and $\Gamma_\sigma = 320$ MeV (Braathen 1972, Petersen and Pisut 1972).

For a consistent set of coupling constants for the coupling to vertices which involve the Δ isobar we rely on the predictions of the quark model (Brown and Weise 1975)

$$f^{*2} = \tfrac{72}{25} f^2 \qquad f^{**2} = \tfrac{1}{25} f^2 \tag{6}$$

for both the π and ρ couplings; this choice is supported by various investigations which predict only slightly different values for the π and ρ coupling to the NΔ and ΔΔ vertices (Sutherland 1967, Michael 1967, Gourdin and Salin 1963).

Figure 2 shows the contributions of the different first-order diagrams (figure 1 (*a*)–(*f*)) to the πNN form factor $F_{\pi\mathrm{NN}}(q^2)$. We see that by far the dominant contribution to our model comes from the $\pi\rho$ triangle diagram figure 1(*b*); all the other diagrams (figures 1 (*c*)–(*f*)) are individually smaller, at least for static pions with not too large momenta ($q \lesssim m_\rho$). In addition, the contributions (*c*) and (*d*) cancel almost exactly. The net effect is a partial compensation of the $\pi\rho$ triangle contribution (*b*) by the pion self-energy diagrams (*e*) and (*f*). The result can be approximated (for $q \lesssim 1$ GeV/*c*) by a monopole form factor with a cut-off mass $\Lambda = 7\, m_\pi$.

Concerning the influence of other agencies, it is found that the contribution from the isobar pole in the various diagrams is in general somewhat smaller than the corresponding N-pole contribution (for the dominant triangle diagram this is demonstrated explicitly in

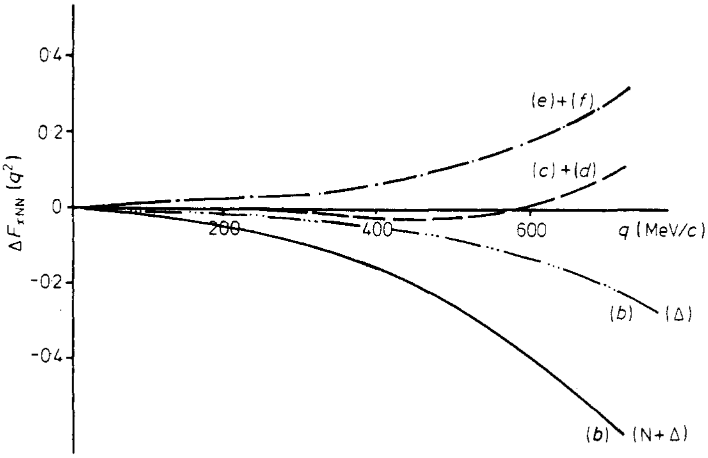

Figure 2. Contributions $\Delta F_{\pi NN}$ of the diagrams (b)–(f) in figure 1 to the πNN form factor plotted against the pion momentum q. For the triangle diagram (b) the contribution from the isobar pole (chain curve, denoted by (Δ)) is compared with the result including both nucleon and isobar excitation (full curve, denoted by (N + Δ)). (The full form factor equals one plus the sum of the contributions shown.)

figure 2), as expected qualitatively from a comparison of the strength and structure of the nucleon and isobar vertices and the corresponding propagators. In addition, we found that the σ exchange plays a negligible role, both in the zero-width and the finite-width approximations, and that the inclusion of the finite ρ width plays no significant role (see also Durso *et al* 1977).

To estimate the influence of higher-order effects, especially from the strongly dominating triangle contributions, we extend our model in the following way. We define an integral equation for $F_{\pi NN}(q^2)$ by introducing the unknown πNN vertex in the triangle diagram itself. For consistency, similar integral equations are then derived for $F_{\pi N\Delta}(q^2)$ and $F_{\pi\Delta\Delta}(q^2)$ as they are all coupled together when the Δ is introduced in the intermediate state. The resulting set of three coupled equations is then solved self-consistently. Explicitly, the coupled system has the following form:

$$F(q^2) = 1 + 8f_\rho \int F(k^2)\delta(\boldsymbol{k},\boldsymbol{q})\mathrm{d}\boldsymbol{k} + \frac{8}{9}\frac{f_\pi^*}{f_\pi} f_\rho^* \int F^*(k^2)\delta^2(\boldsymbol{k},\boldsymbol{q})\,\mathrm{d}\boldsymbol{k} \tag{7a}$$

$$F^*(q^2) = 1 + \frac{f_\pi^*}{f_\pi} f_\rho^* \int F(k^2)\delta(\boldsymbol{k},\boldsymbol{q})\,\mathrm{d}\boldsymbol{k} + 25\frac{f_\pi^{**}}{f_\pi^*} f_\rho^* \int F^{**}(k^2)\delta^*(\boldsymbol{k},\boldsymbol{q})\,\mathrm{d}\boldsymbol{k}$$

$$+f_\rho \int F^*(k^2)\delta(\boldsymbol{k},\boldsymbol{q})\mathrm{d}\boldsymbol{k} + 25 f_\rho^{**} \int F^*(k^2)\delta^*(\boldsymbol{k},\boldsymbol{q})\mathrm{d}\boldsymbol{k} \tag{7b}$$

$$F^{**}(q^2) = 1 + \frac{2}{9}\frac{f_\pi^*}{f_\pi^{**}} f_\rho^* \int F^*(k^2)\delta(\boldsymbol{k},\boldsymbol{q})\mathrm{d}\boldsymbol{k} + 8f_\rho^{**} \int F^{**}(k^2)\delta^*(\boldsymbol{k},\boldsymbol{q})\mathrm{d}\boldsymbol{k} \tag{7c}$$

where

$$F(k^2) \equiv F_{\pi NN}(k^2) \qquad F^*(k^2) \equiv F_{\pi N\Delta}(k^2) \qquad F^{**}(k^2) \equiv F_{\pi\Delta\Delta}(k^2),$$

and $\delta(\boldsymbol{k}, \boldsymbol{q})$ or $\delta^*(\boldsymbol{k}, \boldsymbol{q})$ is the momentum-dependent part of the diagram (figure 1(*b*)) with a nucleon or a Δ in the intermediate state, respectively. (The σ contribution to equations (7*a*–*c*) shows a corresponding structure.)

For the explicit solution of equations (7*a*–*c*) the integration over the intermediate momenta k was truncated around twice the nucleon mass. Since the resulting integral equations in equations (7) are of the Fredholm type with continuous and bounded kernels—as is easily verified—the existence and the uniqueness of the solution is guaranteed (Tricomi 1957; in addition we should note that the consistency of the final result was tested by satisfying the dispersion relation from equation (4)).

Evaluating equations (7*a*–*c*) with the parameters for the σ and ρ meson specified above, we obtain the result shown in figure 3. Inspection indicates that the form factors show a q^2 dependence, which in the low-q^2 region can be reasonably well approximated by the monopole parametrisation in equation (1). Including the pion propagtor corrections from figures 1(*e*) and (*f*) the cut-off masses turn out to be

$$\Lambda_{\pi NN} \simeq 8m_\pi \tag{8a}$$

$$\Lambda_{\pi N\Delta} \simeq 6m_\pi \tag{8b}$$

$$\Lambda_{\pi\Delta\Delta} \simeq 7m_\pi. \tag{8c}$$

Furthermore, the calculation confirms the main features found in the evaluation of the propagator correction, i.e. the strong dominance of ρ exchange and the minor influence of finite-width corrections.

Concerning the quality of the result obtained, a quantitative interpretation is certainly out of the question since various, probably non-negligible, contributions to the vertex function were disregarded in our investigation. Furthermore, significant uncertainties in

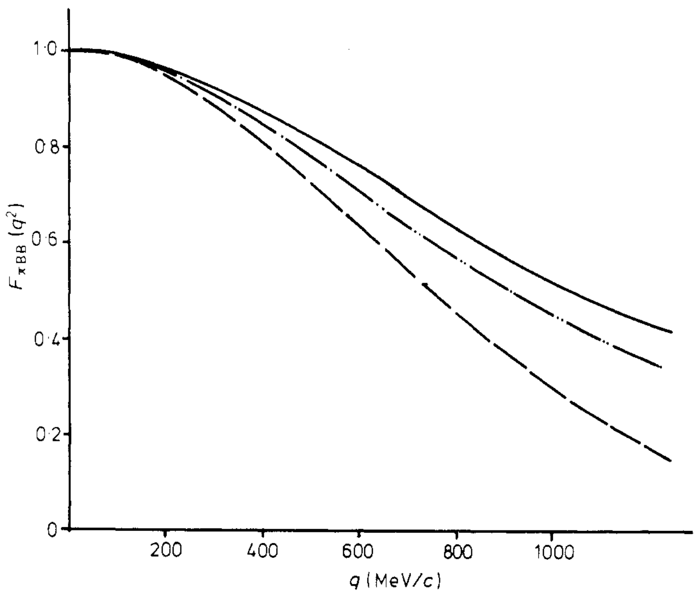

Figure 3. Self-consistent solutions of the integral equations (7*a*–*c*). The full, broken and chain curves denote the πNN, the πNΔ and πΔΔ form factors, respectively, as functions of the pion momentum q.

the coupling constants cannot be excluded at the present time. On the other hand, from the strong dominance of ρ exchange in connection with the very strong ρNN coupling constant ($\kappa \simeq 6$) used in our calculation—which is significantly larger than $\kappa = 3{\cdot}7$ as obtained from vector dominance (Sakurai 1960) and close to the upper limit of ρNN coupling constants floating around (Holinde and Machleidt 1976, Höhler and Pietarinen 1975)—we tend to the interpretation that the numbers in equations (8*a*–*c*) represent lower limits to the cut-off masses. A reduction of the ρNN coupling constant to values conventionally used in OPEP calculations (Bryan and Scott 1969, Erkelenz 1974, Holinde and Machleidt 1976) results in much larger cut-offs, corresponding to a shorter range of the vertex in coordinate space†. To improve this qualitative character of our results, further investigations and a more accurate knowledge of the coupling constants are necessary.

References

Bongardt K *et al* 1974 *Phys. Lett.* **52B** 271
Braathen H J 1972 *Nucl. Phys.* B **44** 93
Brown G E and Weise W 1975 *Phys. Rep.* **22** 281
Bryan R and Scott B 1969 *Phys. Rev.* **177** 1435
Durso J *et al* 1977 *Nucl. Phys.* A **282** 404
Erkelenz K 1974 *Phys. Rep.* **13** 191
Ferrari E and Selleri P 1962 *Nuovo Cim.* **24** 453
Gourdin M and Salin P 1963 *Nuovo Cim.* **27** 305
Höhler J and Pietarinen E 1975 *Nucl. Phys.* B **95** 210
Holinde K and Machleidt R 1976 *Nucl. Phys.* A **256** 479
Iachello F *et al* 1973 *Phys. Lett.* **43B** 191
Mann W A *et al* 1973 *Phys. Rev. Lett.* **31** 844
Michael C 1967 *Phys. Rev.* **156** 1677
Petersen J L and Pisut J 1972 *Nucl. Phys.* B **38** 207
Pagels H 1969 *Phys. Rev.* **179** 1337
——1975 *Phys. Rep.* **16** 221
Sakurai J J 1960 *Ann. Phys., NY* **11** 1
Sutherland D G 1967 *Nuovo Cim.* **48** 188
Tricomi F G 1957 *Integral Equations* (New York: Wiley–Interscience)
Yang C N and Mills R L 1954 *Phys. Rev.* **96** 191

† This sensitivity of the result to the ρNN coupling constant is easily understood if we compare the parametrisation from equation (1) for $\Lambda^2 \gg q^2, m_\pi^2$

$$F_\pi(q^2) = 1 + (q^2/\Lambda^2) + O[(q/\Lambda)^4]$$

with the ansatz in equation (7*a*) which yields immediately $\Lambda \sim f_{\rho NN}^{-1/2}$.